# Development of an OpenFOAM Multiphysics Solver for Solid Fission Products Transport in the Molten Salt Fast Reactor

**Andrea Di Ronco[1], Stefano Lorenzi[1], Francesca Giacobbo[1], Carolina Introini[1], and Antonio Cammi[1]**

[1]Department of Energy, Politecnico di Milano
Via La Masa 34, 20156 Milano, Italy

andrea.dironco@polimi.it, stefano.lorenzi@polimi.it, francesca.giacobbo@polimi.it, carolina.introini@polimi.it, antonio.cammi@polimi.it

*leave space for DOI, which will be inserted by ANS*

## ABSTRACT

The analysis of innovative reactor concepts such as the Molten Salt Fast Reactor (MSFR) requires the development of new modeling and simulation tools. In the case of the MSFR, the strong intrinsic coupling between thermal-hydraulics, neutronics and fuel chemistry has led to the adoption of the multiphysics approach as a state-of-the-art paradigm. One of the peculiar aspects of liquid-fuel reactors such as the MSFR is the mobility of fission products (FPs) in the reactor circuit. Some FP species appear in form of solid precipitates carried by the fuel flow and can deposit on reactor boundaries (e.g., heat exchangers), potentially representing design issues related to the degradation of heat exchange performance or radioactive hotspots. The integration of transport models for solid particles in multiphysics codes is therefore relevant for the prediction of deposited fractions. To this aim, we develop a multiphysics solver based on the OpenFOAM library to address the issue of solid fission products transport. Single-phase incompressible thermal hydraulics are coupled with neutron diffusion, and advection-diffusion-decay equations are implemented for fission products concentrations. Particle deposition and precipitation are considered as well. The developed solver is tested on two different MSFR application to showcase the capabilities of the solver in steady-state simulation and to investigate the role of precipitation and turbulence modeling in the determination of particle concentration distributions.

KEYWORDS: OpenFOAM, multiphysics, molten salt fast reactor, fission products

## 1. INTRODUCTION

The multiphysics approach is becoming a standard one for the development of computational models of the Molten Salt Fast Reactor (MSFR) [1]. The strong coupling among thermal-hydraulics, neutronics and fuel chemistry due to the adoption of circulating fuel requires the development of dedicated simulation tools. Multiphysics codes have been used to study several MSFR features, such as for instance fuel compressibility effects [2], freeze-valve behavior [3] or the estimation of the effective delayed neutron fraction [4]. Among these works, the OpenFOAM library [5] has gained prominence as a reference development platform. The OpenFOAM community is drawing more and more users from the nuclear engineering field and several OpenFOAM-based projects are emerging in recent years [6,7]. OpenFOAM is an open-source C++ library based on the Finite Volume Method which includes an extensive set of physical models, numerical schemes, solution control algorithms, mesh manipulation and post-processing tools and validated solvers for typical problems encountered in CFD.

The aim of this work is to present the development of an OpenFOAM multiphysics solver for the analysis of solid fission products transport in the MSFR. Fission products (FPs) represent a major challenge in

the modeling and design of the MSFR. As they cannot be retained by solid structures, they are free to move through the primary circuit carried by the liquid fuel. Species which are not expected to form stable fluorides within the fuel salt [8] may precipitate as solid particles. Solid FPs are likely to deposit on reactor surfaces, giving rise to potential issues such as formation of localized decay heat sources as well as deterioration of heat exchanger performance. The evaluation of the FPs distribution is also crucial for the estimation of the radiological and decay heat inventory, and for the design of effective removal and reprocessing.

The paper is organized as follows. The developed multiphysics approach is described in Section 2. Two simple applications to showcase the capabilities of the developed solver are shown in Section 3. Conclusive remarks are finally reported in Section 4.

## 2. THE MULTIPHYSICS SOLVER

The solver developed in this work features single-phase incompressible thermal-hydraulics, multi-group neutron diffusion and transport equations for delayed neutron and decay heat precursors. Transport equations for fission products are solved alongside the other physical modules, to provide a fully-coupled multiphysics simulation. All model equations are solved by means of finite-volume discretization, following an iterative segregated coupling approach.

### 2.1. Thermal-hydraulics Model

Continuity, momentum and energy (in temperature form) conservation equations are expressed in a single-phase incompressible formulation:

$$\nabla \cdot \mathbf{u} = 0 \tag{1}$$

$$\frac{\partial \mathbf{u}}{\partial t} + \nabla \cdot (\mathbf{u}\mathbf{u}^T) = -\frac{1}{\rho}\nabla p + \left[1 - \beta_T \left(T - T_0\right)\right] \mathbf{g} + \nabla \cdot \left[\nu_{eff} \left(\nabla \mathbf{u} + (\nabla \mathbf{u})^T\right)\right] \tag{2}$$

$$\frac{\partial T}{\partial t} + \nabla \cdot (\mathbf{u}T) = \nabla \cdot (\alpha_{eff} \nabla T) + \frac{q'''}{\rho c_p} \tag{3}$$

where the quantities $\mathbf{u}$, $p$ and $T$ which correspond to velocity, pressure and temperature, respectively, are intended as averaged in the sense of Reynolds-Averaged Navier-Stokes modeling. It follows that turbulence modeling is performed by means of standard linear eddy-viscosity based closure models, for which effective momentum and thermal diffusivities can be expressed as the sum of a laminar and a turbulent contribution:

$$\nu_{eff} = \nu + \nu_t \tag{4}$$

$$\alpha_{eff} = \alpha + \alpha_t = \frac{\nu}{Pr} + \frac{\nu_t}{Pr_t} \tag{5}$$

where $Pr$ and $Pr_t$ are the Prandtl and turbulent Prandtl numbers, respectively. Momentum and energy equations are coupled thanks to the Boussinesq approximation, for which the density value driving the buoyancy term in Eq. (2) is linearized around a reference temperature $T_0$ and $\beta_T$ represents the volumetric thermal expansion coefficient of the fluid. Except for what concerns density in the linearized buoyancy term, constant average values are used for thermophysical properties to keep the numerics and the coupling between different physics as simple as possible. Finally, $q'''$ represents a volumetric energy source which includes internal heat generation - both prompt and delayed, see Eq. (10) - and optionally other energy sinks to model heat removal mechanisms.

### 2.2. Neutronics Model

The multi-group diffusion model is adopted for neutron flux calculations [9]. Despite some limitations, it is widely employed in standard nuclear reactor analysis. Thanks to its relative simplicity and limited computational effort, it has found several successful applications especially for multiphysics analysis [10,11]. The diffusion equation for the $g$-th group-integrated neutron flux $\varphi_g$ reads:

$$\frac{1}{v_g}\frac{\partial \varphi_g}{\partial t} = \nabla \cdot (D_{n,g} \nabla \varphi_g) - \Sigma_{a,g}\,\varphi_g - \sum_{h \neq g} \Sigma_{s,g\to h}\,\varphi_g + (1-\beta_d)\,\chi_{p,g}\,\frac{\bar{\nu}_g}{k_{eff}}\,\Sigma_{f,g}\,\varphi_g + S_{n,g} \tag{6}$$

where $S_{n,g}$ is the explicit neutron source of the $g$-th group, constituted by prompt fission and scattering neutrons from other groups and delayed neutron precursors decay:

$$S_{n,g} = (1-\beta_d) \sum_{h \neq g} \chi_{p,h}\,\frac{\bar{\nu}_h}{k_{eff}}\,\Sigma_{f,h}\,\varphi_h + \sum_{h \neq g} \Sigma_{s,h\to g}\,\varphi_h + \chi_{d,h} \sum_k \lambda_{d,k} c_k \tag{7}$$

It is worth mentioning that $k_{eff}$ acts as a tunable multiplication factor to model a prescribed reactivity insertion. A power-iteration routine for the solution of the k-eigenvalue problem is also included for steady-state simulation, which allows for the iterative adjustment of $k_{eff}$ to attain criticality at a specified power level.

Due to the circulating nature of the fuel, transport equations are formulated also for delayed neutron and decay heat precursors. The transport equation for the concentration of delayed neutron precursors of the $k$-th family $c_k$ reads:

$$\frac{\partial c_k}{\partial t} + \nabla \cdot (\mathbf{u}\, c_k) = \nabla \cdot (D_{eff}\,\nabla c_k) - \lambda_{d,k}\, c_k + \beta_{d,k} \sum_g \bar{\nu}_g\,\Sigma_{f,g}\,\varphi_g \tag{8}$$

An analogous equation holds for the concentration of decay heat precursors of the $l$-th family $d_l$:

$$\frac{\partial d_l}{\partial t} + \nabla \cdot (\mathbf{u}\, d_l) = \nabla \cdot (D_{eff}\,\nabla d_l) - \lambda_{h,l}\, d_l + \beta_{h,l} \sum_g \bar{E}_{f,g}\,\Sigma_{f,g}\,\varphi_g \tag{9}$$

In the above equation, the actual concentration of decay heat precursors is multiplied by the average fission energy, such that $d_l$ represents a volumetric amount of "latent" fission energy. Consistently, the volumetric heat source is given by:

$$q''' = (1-\beta_h) \sum_g \bar{E}_{f,g}\,\Sigma_{f,g}\,\varphi_g + \sum_l \lambda_{h,l}\, d_l \tag{10}$$

For what concerns the diffusive transport of delayed neutrons and decay heat precursors, the diffusion coefficient $D_{eff}$ is simply defined in analogy with momentum and thermal diffusivities:

$$D_{eff} = D + D_t = \frac{\nu}{Sc} + \frac{\nu_t}{Sc_t} \tag{11}$$

where $Sc$ and $Sc_t$ are the Schmidt and turbulent Schmidt numbers, respectively.

Group constants are adjusted as functions of local temperature around reference values to account for Doppler and fuel density effects. For a generic neutron reaction $r$ occurring in the $g$-th energy group:

$$\Sigma_{r,g} = \left(\Sigma^0_{r,g} + A^0_{r,g}\,\log\frac{T}{T_0^\Sigma}\right)\frac{1-\beta_T\,(T-T_0)}{1-\beta_T(T_0^\Sigma - T_0)} \tag{12}$$

where Doppler effects are modeled by means of a logarithmic term where $\Sigma^0_{r,g}$ and $A^0_{r,g}$ respectively represent the cross-section and a corresponding logarithmic coefficient at a reference temperature $T_0^\Sigma$, whereas density effects are taken into account through a linear correction consistently with the buoyancy term. The reference temperature for cross-sections can be chosen independently from $T_0$. An analogous approach is employed for the correction of the neutron diffusion coefficients $D_{n,g}$. The quantities $\Sigma^0_{r,g}$ and $A^0_{r,g}$ are evaluated by means of the Monte Carlo reactor physics and burnup code SERPENT 2 [12].

### 2.3. Fission Products Model

Each fission product specie is modeled as a continuous scalar concentration field subject to advection, dispersion and decay mechanisms:

$$\frac{\partial f_i}{\partial t} + \nabla \cdot (\mathbf{u}\, f_i) = \nabla \cdot (D_{eff} \nabla f_i) - \lambda_i\, f_i + y_i \sum_g \Sigma_{f,g}\, \varphi_g \tag{13}$$

where $f_i$ represents the concentration of the $i$-th solid fission product species under consideration, expressed in number of particles per unit volume. As far as transport is concerned, we neglect chemical interactions and formation of separate phases and the source term is simply related to the fission rate through a suitable yield coefficient $y_i$.

The single-phase Eulerian approach is employed to limit the additional complexity of the computational model. It represents a valid approximation in many cases of interest, provided that particles are sufficiently small and do not interact among themselves [13]. Previous experience with MSRs [14] suggests the validity of such modeling choice, at least at a first degree of approximation. The particle size can be used to derive a common expression for the laminar diffusivity $D$, which is given by the Einstein equation:

$$D = \frac{k_B T}{3\pi \rho \nu d_p} \tag{14}$$

where $k_B$ is the Boltzmann constant and $d_p$ is the particle diameter. The above equation is derived under the assumption of large Schmidt number $Sc$ [15] and can be used to estimate $Sc$ in such limit. For more details and for a first assessment of this modeling approach we refer to [16].

#### 2.3.1. Particle deposition

Particle-wall interaction mechanisms can be modeled separately from the bulk flow. This approach, which is valid under fairly general hypotheses on the nature of particle-wall interactions, assumes that relevant interactions only occur in a thin wall region whose influence can be collapsed in a first-order boundary conditions for the bulk flow [17]:

$$-D_{eff} \nabla f_i \cdot \mathbf{n} = \gamma\, f_i \tag{15}$$

for any point on the wall boundary, where $\mathbf{n}$ denotes the outward pointing wall-normal direction. In this model, wall adsorption of FP particles is modeled through a single deposition parameter $\gamma$, which has the physical dimensions of a velocity. In this work, we adopt the assumption of "perfectly adsorbing" walls, i.e. we let $\gamma$ tend to infinite such that the wall boundary condition simplifies to

$$f_i = 0 \tag{16}$$

In this way, conservative estimates of deposition fluxes are obtained. This represents indeed a major approximation, but it is widely adopted in the literature of CFD-based particle transport problems. Moreover, system-code approaches which follow fluid dynamic analogy with momentum transport are in general not feasible due to non-standard geometries found in MSFR cases.

#### 2.3.2. Precipitation chemistry

Solid FPs are constituted by "noble metal" species (Mo, Rh, Ru, Pd, Tc and possibly others) which are expected to be normally found exclusively in solid precipitate phase within the chemical environment of the MSFR [18]. Presence of solute should be negligible in most cases, but temperature-dependent coexistence with precipitate might be relevant in particular circumstances such as accidental scenarios. In this work, we consider the implementation of a simplified equilibrium thermochemistry model. Albeit simple, this approach can mimic the effects due to local temperature. More advanced approaches can be considered

as well, such as the coupling with external thermochemistry codes [19]. The local equilibrium hypothesis allows for the solution of algebraic constraint equations instead of altering the differential transport equations with stiff non-linear reaction terms. Following common practice in CFD-thermochemistry coupling for reactive transport problems [20], a segregated approach using temperature-dependent linear equilibrium constraints has been selected. A simple precipitation-dissolution reaction involving single metallic species is considered

$$M + nUF_4 \rightleftharpoons MF_n + nUF_3 \tag{17}$$

$$\left[M^{n+}\right] = K(T)\left(\frac{\left[U^{4+}\right]}{\left[U^{3+}\right]}\right)^n \tag{18}$$

where $M$ denotes a generic metallic species and square brackets indicate concentrations (we assume for simplicity that chemical activity coincides with concentration). The $UF_4$-to-$UF_3$ ratio can be considered as a design parameter and in in this work we assume a value of 100. For simplicity, we can assume the stoichiometric coefficient $n$ equal to 1. Following this approach, the particle concentration $f_i$ can be split into precipitated and dissolved contributions:

$$f_i = f_i^p + f_i^s \tag{19}$$

where, in this context, $f_i^s$ coincides with $[M^{n+}]$ up to a multiplicative constant. The temperature dependence of the equilibrium constant $K(T)$ is assumed exponential, following a standard Van 't Hoff equation:

$$\log\frac{K(T_2)}{K(T_1)} = \frac{\Delta H^0}{R}\left(\frac{1}{T_1} - \frac{1}{T_2}\right) \tag{20}$$

where $\Delta H^0$ denotes a standard reaction enthalpy and $R$ is the universal gas constant.

## 3. APPLICATIONS

In this section, two separate steady-state applications to showcase the capabilities of the developed solved. In the first case, a laminar two-dimensional case is used to demonstrate the effect of precipitation on the distribution of solid particles. In the second, we setup a turbulent case to show the distribution of fission products in a steady-state MSFR simulation. Both cases are selected for their simplified geometric features, which enable the production of high-quality numerical grids even when wall refinement is crucial for the resolution of particle transport in the wall regions. Furthermore, the adoption of two-dimensional cases allows for a significant reduction of computational requirements.

### 3.1. Precipitation in the Lid-driven Cavity Benchmark Case

The lid-driven cavity was recently employed to develop a reference case for a numerical benchmark of different multiphysics MSFR codes. A detailed description of the case and of the benchmark procedure can be found in [1]. The domain is characterized by a 2 m by 2 m cavity filled with molten salt. The domain is treated as a homogeneous, bare reactor. Therefore, standard vacuum conditions are applied for the neutron flux to each boundary, together with a homogeneous Neumann condition for the delayed neutron precursors. Decay heat precursors are not simulated in this case, for better consistence with [1]. The driving force for the liquid fuel flow is given by the upper lid, which moves at constant velocity of 0.5 m $s^{-1}$. All walls are treated as adiabatic, while energy is removed from the system through a simple volumetric heat sink:

$$q_r''' = -\frac{\gamma_r}{V_r}(T - T_{sink}) \tag{21}$$

where $\gamma_r$ is a total heat removal coefficient and $V_r$ is the volume of heat removal region, which in this case coincides with the entire cavity domain. The main case parameters are summarized in Table I. Being the analysis conducted in steady-state conditions, simulations are performed in criticality eigenvalue mode with

the integrated power normalized to 1000 MW. For what concerns the equilibrium constants, the following guess values are used: $K(T_1)$ = $10^{-6}$ and $K(T_2)$ = $10^{-5}$ with $T_1$ and $T_2$ equal respectively to 1000 K and 1200 K.

Fig. 1 shows the comparison between a base case where no equilibrium precipitation-dissolution reaction is considered and all FP atoms are born directly as precipitate and the case with chemical model with parameter values as described earlier. Non-negligible discrepancies are observed, suggesting that even in a simplified test case temperature-dependent effects on precipitation may sensibly affect precipitate distributions within the reactor.

**Table I: Main physical parameter values adopted for the lid-driven cavity case [1]**

| Parameter | Symbol | Units | Value |
|---|---|---|---|
| Lid velocity | $U$ | m $s^{-1}$ | 0.5 |
| Density | $\rho$ | kg $m^{-3}$ | $2.0\times10^{3}$ |
| Kinematic viscosity | $\nu$ | $m^2$ $s^{-1}$ | $2.5\times10^{-2}$ |
| Specific heat capacity | $c_p$ | J $kg^{-1}$ $K^{-1}$ | $3.075\times10^{3}$ |
| Thermal expansion coeff. | $\beta_T$ | $K^{-1}$ | $2.0\times10^{-4}$ |
| Ref. temperature | $T_0$ | K | 900 |
| Prandtl number | $Pr$ | - | $3.075\times10^{5}$ |
| Schmidt number | $Sc$ | - | $2.0\times10^{8}$ |
| Heat removal coeff. | $\gamma_r$ | W $K^{-1}$ | $4.0\times10^{6}$ |
| Heat sink temperature | $T_{sink}$ | K | 900 |
| Decay constant | $\lambda$ | $s^{-1}$ | $10^{-5}$ |
| Fission yield | $y$ | - | $10^{-2}$ |

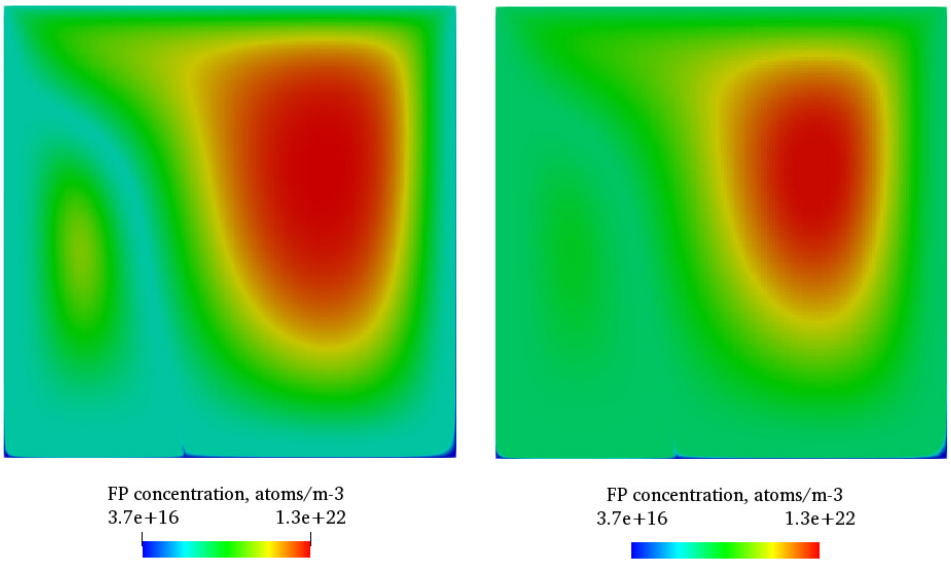


**Figure 1: FP precipitate concentration $f^p$ for the cavity benchmark case. On the left, base case with direct formation of the solid precipitate phase; on the right, simplified equilibrium precipitation model**

### 3.2. Turbulent Transport in a 2D MSFR Case

A simplified two-dimensional axisymmetric MSFR geometry is adopted. It features the loop structure typical of the MSFR with fuel recirculation, allowing for the simulation of more realistic turbulent cases even in a simplified setup. The heat exchanger is modeled similarly as in the cavity case, through the use of a linear sink term analogous to Eq. (21). The heat removal coefficient $\gamma_r$ is here assumed to be zero outside the heat exchanger region. For what concerns the pump, a momentum source is imposed, along the vertical direction, which matches the flow rate at the pump outlet section to the total one ($1.9\times10^4$ kg s$^{-1}$, for the entire reactor). The main physical case parameters are summarized in II. Also in this case the analysis is in steady-state and power iteration is used to achieve criticality at a power lever which corresponds to 3000 MW for the entire reactor.

Two different steady-state cases are simulated to assess the effect of turbulence modeling on the transport of FP particles. The solver makes use of the standard linear eddy viscosity approach for the modeling of turbulent quantities and for these cases the standard $k$-$\varepsilon$ turbulence model [21] is used. The two simulated cases correspond to different values of the turbulent Schmidt number $Sc_t$, 0.50 and 1.20. Gradient-based turbulent diffusion constitutes a standard approach in CFD and multiphysics analysis, but relies heavily on the turbulent Schmidt number $Sc_t$, with optimal values depending on fluid properties and on flow configuration [22].

Fig. 2 shows the comparison between FP precipitate concentration fields in the two simulated cases. Significant differences can be observed, suggesting that the choice of the turbulent Schmidt number appears to play a relevant role in the transport of solid fission products. Larger values lead to lower diffusivities and increased precipitate concentrations, as evidenced in the results.

**Table II: Main physical parameter values adopted for the 2D axisymmetric MSFR case**

| | | | |
|---|---|---|---|
| Density | $\rho$ | kg m$^{-3}$ | $4.307\times10^{3}$ |
| Kinematic viscosity | $\nu$ | m$^2$ s$^{-1}$ | $5.89\times10^{-6}$ |
| Specific heat capacity | $c_p$ | J kg$^{-1}$ K$^{-1}$ | $1.594\times10^{3}$ |
| Thermal expansion coeff. | $\beta_T$ | K$^{-1}$ | $1.912\times10^{-4}$ |
| Ref. temperature | $T_0$ | K | 973 |
| Prandtl number | $Pr$ | - | 23.78 |
| Turb. Prandtl number | $Pr_t$ | - | 0.85 |
| Schmidt number | $Sc$ | - | 20.0 |
| Turb. Schmidt number | $Sc_t$ | - | 0.50/0.85/1.20 |
| Heat removal coeff. | $\gamma_r$ | W m$^{-2}$ K$^{-1}$ | $2.5\times10^{6}$ |
| Heat sink temperature | $T_{sink}$ | K | 900 |
| Decay constant | $\lambda$ | s$^{-1}$ | $10^{-5}$ |
| Fission yield | $y$ | - | $10^{-2}$ |

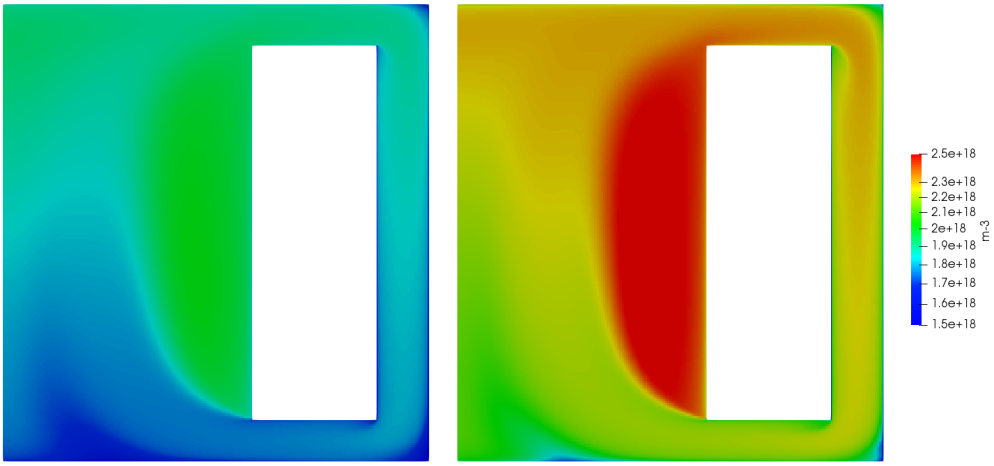


**Figure 2: FP precipitate concentration $f^p$ distributions for the $k-\varepsilon$ turbulence model. Left and right plots correspond to $Sc_t$ equal to 0.50 and 1.20, respectively**

## 4. CONCLUSIONS

In this paper, we presented a multiphysics solver for the analysis of solid fission products transport in the Molten Salt Fast Reactor, based on the OpenFOAM library. The solver features incompressible single-phase thermal-hydraulics and neutron diffusion coupled with transport of precursors of delayed neutrons and decay heat. Solid fission products are modeled, according to the single-phase approach, as transported quantities which obey to advection-diffusion-decay equations. Particle deposition on walls is modeled by

means of the "perfectly adsorbing" walls assumption, while temperature-dependent effects on precipitation are determined by a simple equilibrium precipitation-dissolution reaction model.

The developed solver is tested on two separate molten salt cases, namely the lid-driven cavity problem and a two-dimensional MSFR geometry. Results from these simple applications show a non-negligible role of precipitation modeling and of the choice of turbulent dispersion parameters on the distribution of solid precipitate particles, suggesting the need for further study. Despite relevant for the analysis of MSFR behavior, the adopted geometries were selected to simplify the numerical analysis and to reduce the computational requirements. Future work will include the analysis of FPs transport in more realistic 3D reactor simulations. Other possible extensions of the present work might include the adoption of more sophisticated turbulence modeling approaches such as Large Eddy Simulation. As a long-term development goal, direct coupling of OpenFOAM MSFR solvers with the external equilibrium thermochemistry code Thermochimica [23] is foreseen, to allow for a more accurate description of precipitation/dissolution phenomena within the fuel.

## ACKNOWLEDGEMENTS

This project has received funding from the Euratom research and training programme 2014-2018 under grant agreement no. 847527. This work was partly motivated by the IAEA Open-source Nuclear Codes for Reactor Analysis (ONCORE) initiative, a collaborative framework for the development and application of open-source multi-physics to support research, education, and training in nuclear science and technology.

## REFERENCES

[1] M. Tiberga, R. G. G. de Oliveira, E. Cervi, J. A. Blanco, S. Lorenzi, M. Aufiero, D. Lathouwers, and P. Rubiolo. "Results from a multi-physics numerical benchmark for codes dedicated to molten salt fast reactors." *Annals of Nuclear Energy*, **volume 142**, p. 107428 (2020).

[2] E. Cervi, S. Lorenzi, A. Cammi, and L. Luzzi. "Development of a multiphysics model for the study of fuel compressibility effects in the Molten Salt Fast Reactor." *Chemical Engineering Science*, **volume 193**, pp. 379–393 (2019).

[3] M. Tiberga, D. Shafer, D. Lathouwers, M. Rohde, and J. L. Kloosterman. "Preliminary investigation on the melting behavior of a freeze-valve for the Molten Salt Fast Reactor." *Annals of Nuclear Energy*, **volume 132**, pp. 544–554 (2019).

[4] M. Aufiero, M. Brovchenko, A. Cammi, I. Clifford, O. Geoffroy, D. Heuer, A. Laureau, M. Losa, L. Luzzi, E. Merle-Lucotte, M. E. Ricotti, and H. Rouch. "Calculating the effective delayed neutron fraction in the Molten Salt Fast Reactor: Analytical, deterministic and Monte Carlo approaches." *Annals of Nuclear Energy*, **volume 65**, pp. 78–90 (2014).

[5] The OpenFOAM Foundation. "OpenFOAM v9 User Guide." URL https://cfd.direct/openfoam/user-guide.

[6] C. Fiorina, I. Clifford, M. Aufiero, and K. Mikityuk. "GeN-Foam: a novel OpenFOAM® based multi-physics solver for 2D/3D transient analysis of nuclear reactors." *Nuclear Engineering and Design*, **volume 294**, pp. 24–37 (2015).

[7] C. Fiorina, I. Clifford, S. Kelm, and S. Lorenzi. "On the development of multi-physics tools for nuclear reactor analysis based on OpenFOAM®: state of the art, lessons learned and perspectives." *Nuclear Engineering and Design*, **volume 387**, p. 111604 (2022).

[8] C. Baes. "The chemistry and thermodynamics of molten salt reactor fuels." *Journal of Nuclear Materials*, **volume 51**(1), pp. 149–162 (1974).

[9] A. Hébert. "Multigroup neutron transport and diffusion computations." In D. G. Cacuci, editor, *Handbook of Nuclear Engineering*, pp. 751–911. Springer US, Boston, MA (2010).

[10] C. Fiorina, M. Aufiero, A. Cammi, C. Guerrieri, J. Krepel, L. Luzzi, K. Mikityuk, and M. Ricotti. "Analysis of the MSFR core neutronics adopting different neutron transport models." In *International Conference on Nuclear Engineering, Proceedings, ICONE*, volume 5 (2012).

[11] C. Fiorina, N. Kerkar, K. Mikityuk, P. Rubiolo, and A. Pautz. "Development and verification of the neutron diffusion solver for the GeN-Foam multi-physics platform." *Annals of Nuclear Energy*, **volume 96**, pp. 212–222 (2016).

[12] J. Leppänen, M. Pusa, T. Viitanen, V. Valtavirta, and T. Kaltiaisenaho. "The Serpent Monte Carlo code: Status, development and applications in 2013." *Annals of Nuclear Energy*, **volume 82**, pp. 142–150 (2015).

[13] A. Guha. "Transport and Deposition of Particles in Turbulent and Laminar Flow." *Annual Review of Fluid Mechanics*, **volume 40**(1), pp. 311–341 (2008).

[14] E. Compere, S. Kirslis, E. Bohlmann, F. Blankenship, and W. Grimes. "Fission product behavior in the molten salt reactor experiment." Technical Report ORNL–4865, 4077644, Oak Ridge National Laboratory (1975).

[15] F. Balboa Usabiaga, X. Xie, R. Delgado-Buscalioni, and A. Donev. "The Stokes-Einstein relation at moderate Schmidt number." *The Journal of Chemical Physics*, **volume 139**(21), p. 214113 (2013).

[16] A. Di Ronco, S. Lorenzi, F. Giacobbo, and A. Cammi. "An Eulerian Single-Phase Transport Model for Solid Fission Products in the Molten Salt Fast Reactor: Development of an Analytical Solution for Verification Purposes." *Frontiers in Energy Research*, **volume 9**, p. 692627 (2021).

[17] D. C. Prieve and E. Ruckenstein. "Rates of deposition of brownian particles calculated by lumping interaction forces into a boundary condition." *Journal of Colloid and Interface Science*, **volume 57**(3), pp. 547–550 (1976).

[18] O. Beneš and R. Konings. "Molten Salt Reactor Fuel and Coolant." In R. J. Konings, editor, *Comprehensive Nuclear Materials*, pp. 359–389. Elsevier, Oxford (2012).

[19] A. Marino, M. Peltomäki, J. Lim, and A. Aerts. "A multi-physics computational tool based on CFD and GEM chemical equilibrium solver for modeling coolant chemistry in nuclear reactors." *Progress in Nuclear Energy*, **volume 120**, p. 103190 (2020).

[20] J. Carrayrou, R. Mosé, and P. Behra. "Operator-splitting procedures for reactive transport and comparison of mass balance errors." *Journal of Contaminant Hydrology*, **volume 68**(3), pp. 239–268 (2004).

[21] B. Launder and D. Spalding. "The numerical computation of turbulent flows." *Computer Methods in Applied Mechanics and Engineering*, **volume 3**(2), pp. 269–289 (1974).

[22] Y. Tominaga and T. Stathopoulos. "Turbulent Schmidt numbers for CFD analysis with various types of flowfield." *Atmospheric Environment*, **volume 41**(37), pp. 8091–8099 (2007).

[23] M. Piro, S. Simunovic, T. Besmann, B. Lewis, and W. Thompson. "The thermochemistry library Thermochimica." *Computational Materials Science*, **volume 67**, pp. 266–272 (2013).